Supplementary Figure 1.

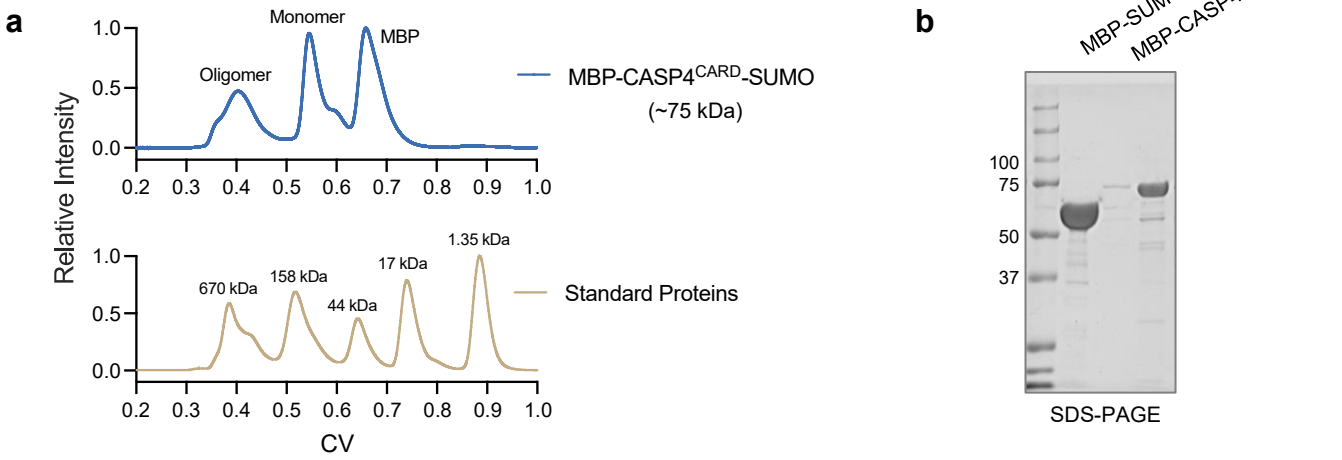

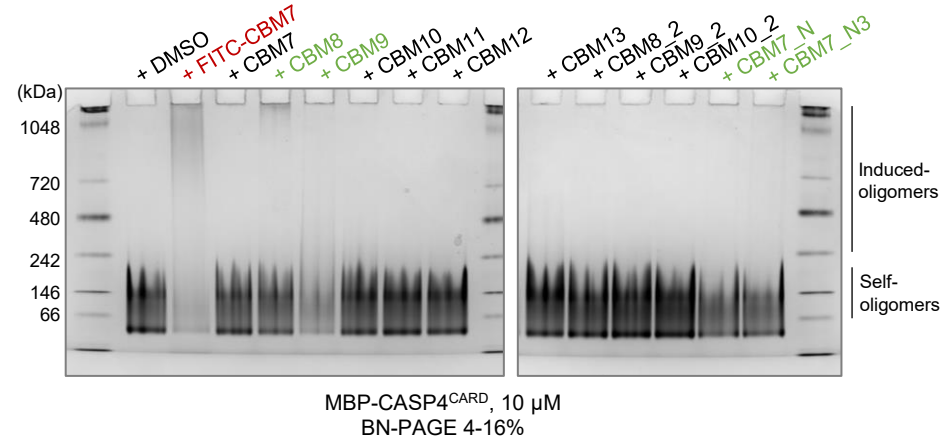

d

Peptide	Sequence
FITC-CBM7	FITC-Ahx-FLFFIRH
CBM7	FLFFIRH
CBM8	PFLFFIRH
CBM9	HPFLFFIRH
CBM10	DHPFLFFIRH
CBM11	ADHPFLFFIRH
CBM12	TADHPFLFFIRH
CBM13	FTADHPFLFFIRH
CBM8_2	FLFFIRHN
CBM9_2	FLFFIRHNS
CBM10_2	FLFFIRHNSS
CBM7_N	WFLFFIRH
CBM7_N3	WDGFLFFIRH

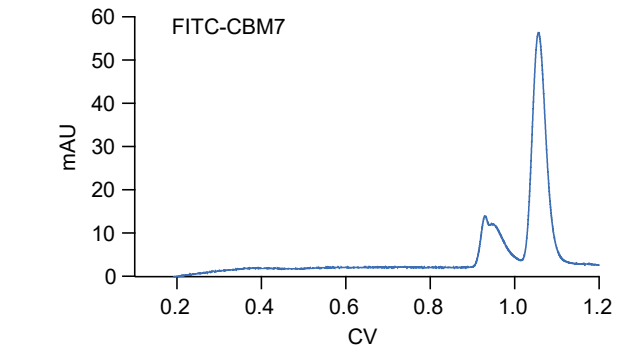

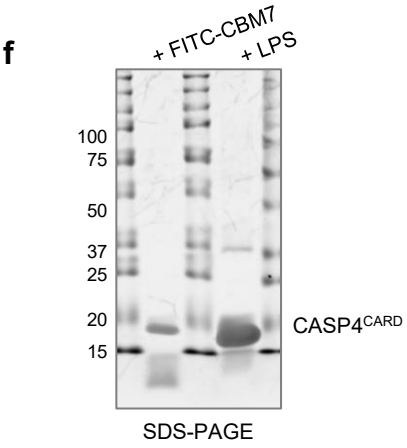

Supplementary Figure 1. **a**. SEC profile of *E. coli* expressed MBP-CASP4^{CARD}-SUMO aligned with molecular-weight standard proteins. **b**. SDS-PAGE analysis of MBP-SUMO and monomeric MBP-CASP4^{CARD}-SUMO fractions collected after SEC. **c**. BN-PAGE analysis of MBP-CASP4^{CARD} oligomerization in the presence of CBM7 and derivative peptides, with a protein-to-peptide molar ratio 1:5. **d**. Sequence information of all peptides tested in panel (c). **e**. SEC profile of FITC-CBM7 alone. **f**. SDS-PAGE analysis of oligomeric fractions collected from SEC experiments shown in Fig. 1f.

Supplementary Figure 2.

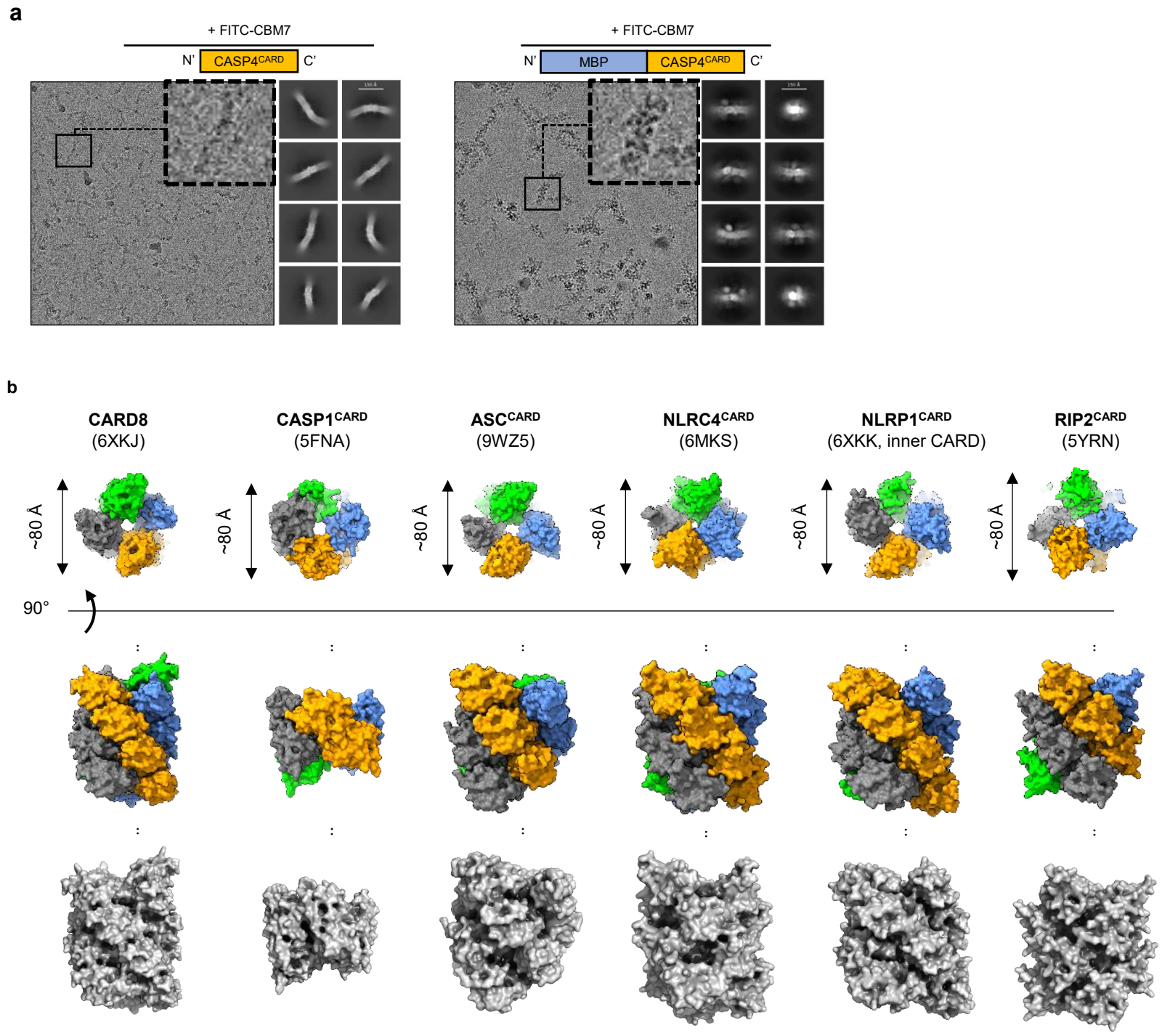

Supplementary Figure 2. Structural comparison of CARD oligomers. **a**. Representative motion-corrected cryoEM micrographs and 2D classification result of FITC-CBM7-induced CASP4^{CARD} assemblies with or without MBP fusion. **b.** Top and side views of six previously characterized CARD filament structures. In the side views, the upper panel is color-coded to illustrate filament assembly organization, whereas the lower panel highlights cleft regions formed within the assemblies.

Supplementary Figure 3.

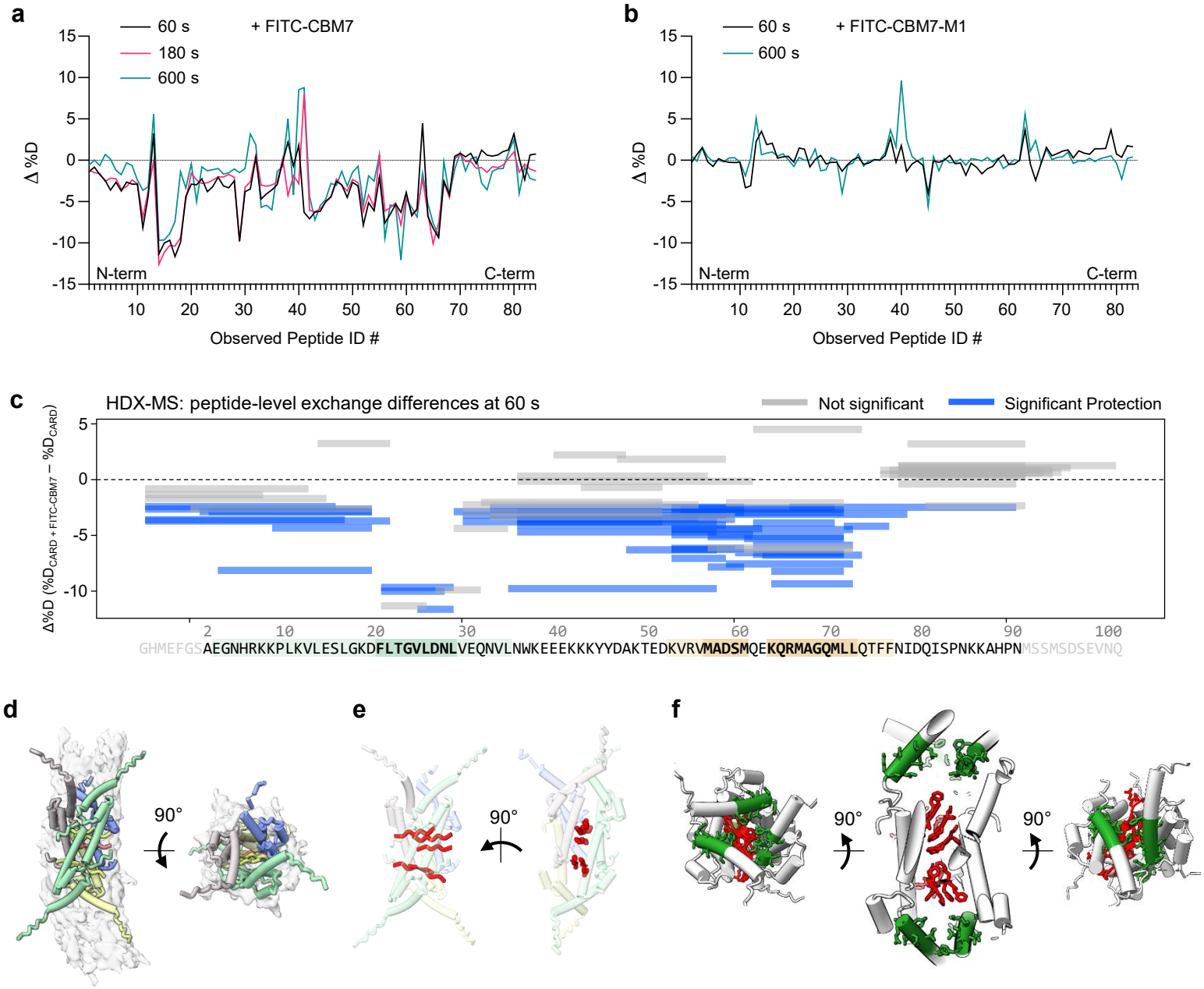

Supplementary Figure 3. a-b. Peptide-level deuterium uptake differences over time, between FITC-CBM7-bound and apo CASP4^{CARD} (a), or between FITC-CBM7-M1-bound and apo CASP4^{CARD} (b). **c**. The Woods plot of peptide-level deuterium uptake differences between FITC-CBM7-bound and apo CASP4^{CARD} at 60 s exchange. **d.** Superposition of the AlphaFold prediction model with the *ab initio* cryoEM reconstruction of the CASP4^{CARD} oligomer. The AlphaFold model is shown as a cartoon and the *ab initio* cryoEM map as a transparent surface. Side and top views are presented. **e**. Location of the CBM7 peptide (red) on the AlphaFold prediction model of the CASP4^{CARD} oligomer. Side and top views are shown. **f**. Orthogonal views of the proposed structural model showing the spatial relationship between the FITC-CBM7 peptide (red) and CASP4^{CARD} residues 21-29 (green).

Supplementary Figure 4.

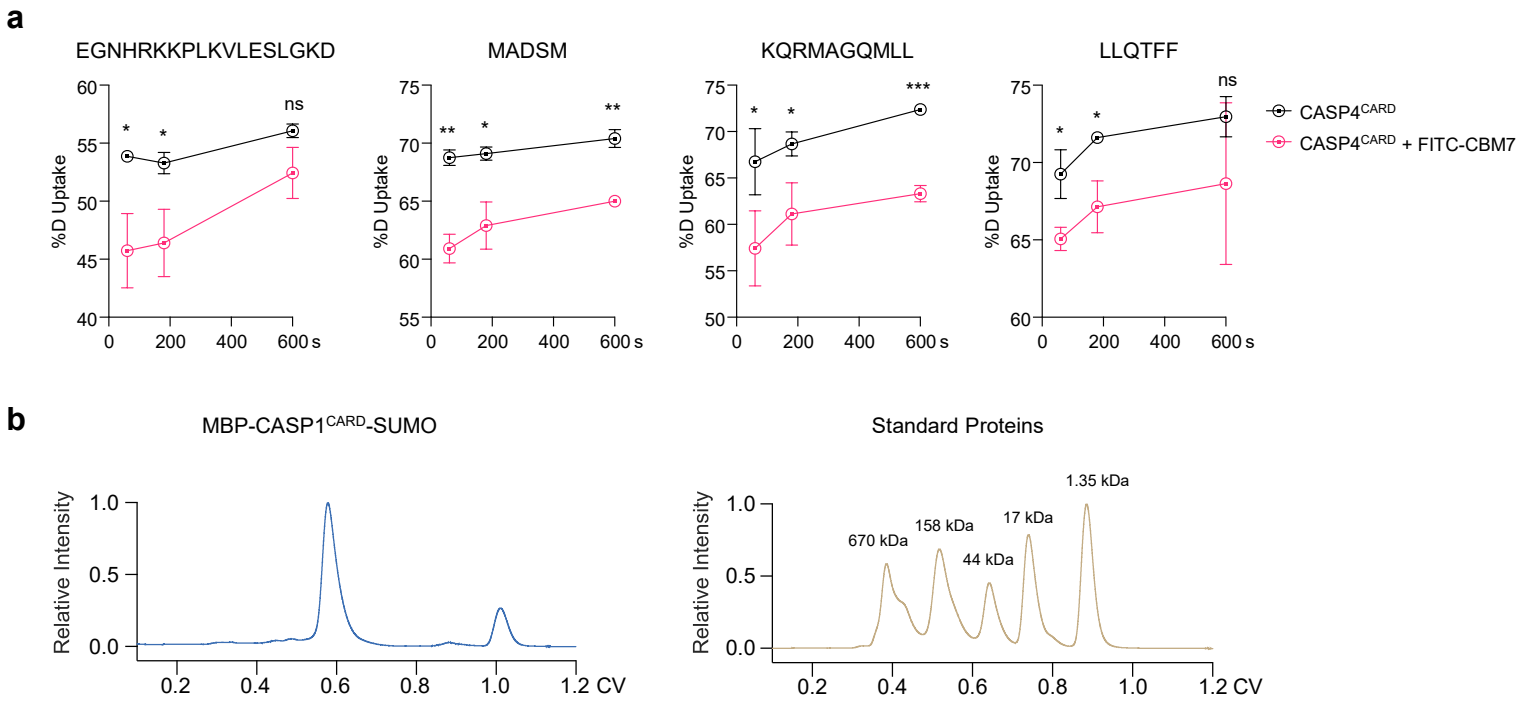

Supplementary Figure 3. a. Selected observed peptides deuterium uptake over time in addition to Fig 2g. Data are presented as mean ± S.D. Statistical significance is indicated. **b**. SEC profile of MBP-CASP1^{CARD}-SUMO (left) and molecular-weight standards (right).

Supplementary Figure 5.

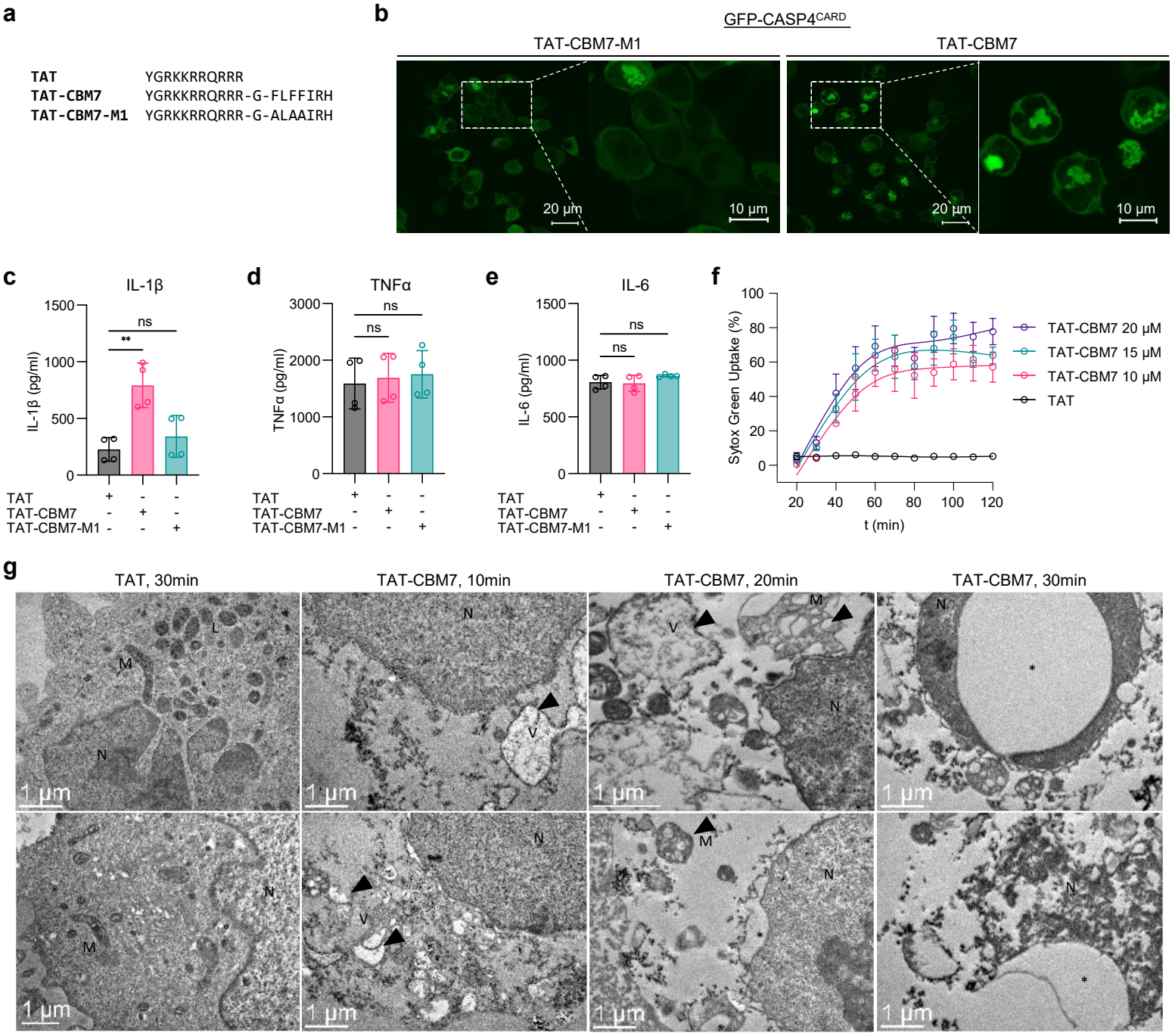

Supplementary Figure 5. a. sequence information of peptides used in cellular studies. A glycine is inserted in between TAT and CBM7 as a spacer. **b**. Higher-magnification of GFP-CASP4^{CARD} puncta formation that are with the same condition as Fig. 4a. **c-e**. IL-1β, TNF-α, and IL-6 secretion from THP-1 macrophages treated with indicated peptides. One-way ANOVA was performed for statistical significance. **f**. Time-course analysis of plasma-membrane permeabilization using Sytox Green uptake in U937 monocytes treated with peptides. **g**. Additional TEM images corresponding to Fig. 5b.

Supplementary Figure 6.

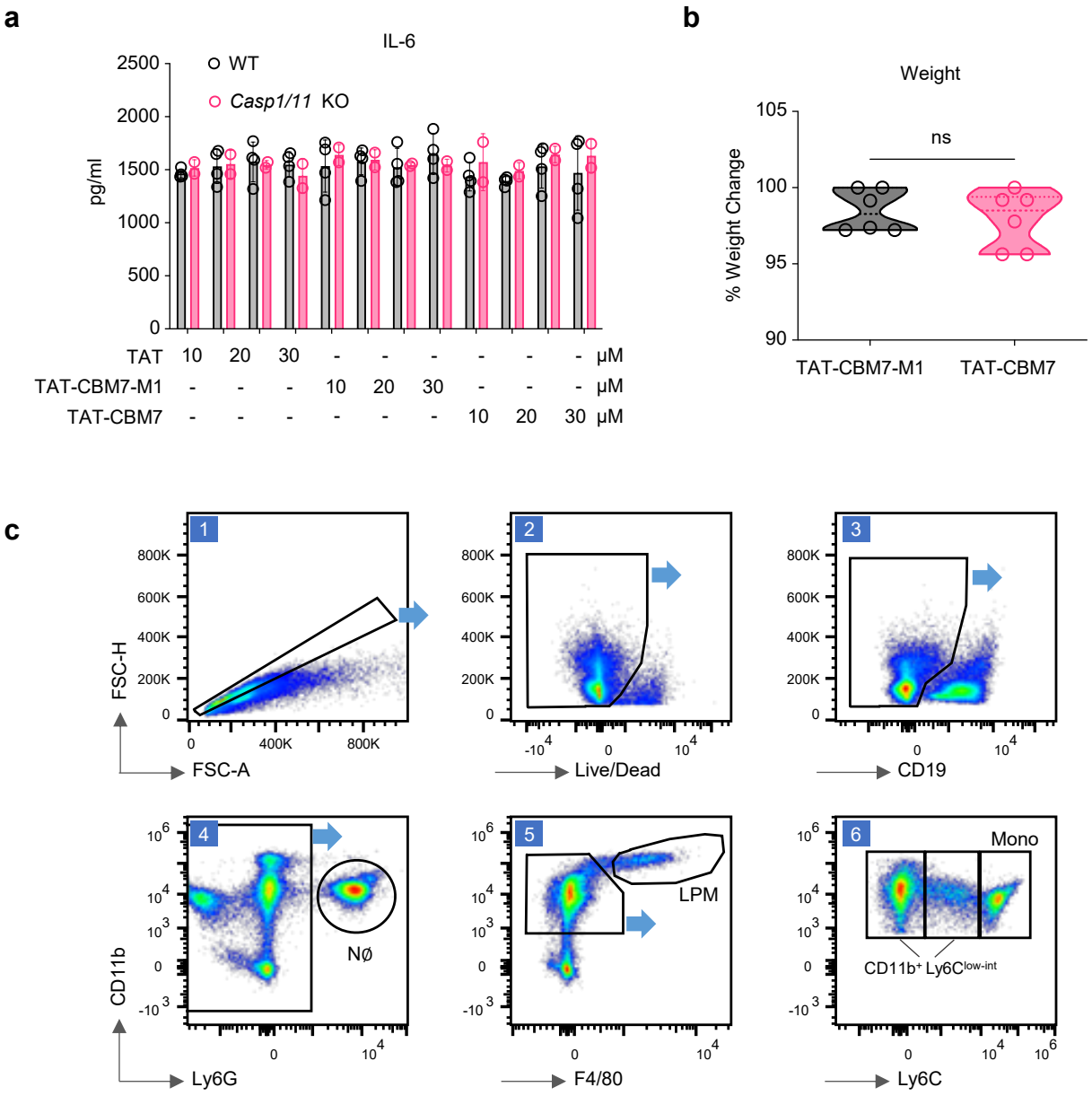

Supplementary Figure 6. a. IL-6 cytokine secretion from BMDMs treated as in Fig. 6a. **b**. Body-weight changes of mice 1 day post peptide injection. **c**. Flow-cytometry gating strategy for peritoneal immune-cell populations.